Original Article

Association between pre-procedural computed tomography angiography-based global longitudinal strain and outcomes in patients undergoing transcatheter aortic valve implantation

Yan-Chun Chen[1#], Yi-Feng Gao[1#], Zhen Zhou[1], Kai-Rui Bo[1], Guang-Yuan Song[2], Lei Xu[1]

[1]Department of Radiology, Beijing Anzhen Hospital, Capital Medical University, Beijing, China; [2]Interventional Center of Valvular Heart Disease, Beijing Anzhen Hospital, Capital Medical University, Beijing, China

Contributions: (I) Conception and design: YC Chen, L Xu; (II) Administrative support: GY Song; (III) Provision of study materials or patients: YF Gao; (IV) Collection and assembly of data: YC Chen, Z Zhou; (V) Data analysis and interpretation: YC Chen, KR Bo; (VI) Manuscript writing: All authors; (VII) Final approval of manuscript: All authors.

[#]These authors contributed equally to this work as co-first authors.

Correspondence to: Lei Xu, MD. Department of Radiology, Beijing Anzhen Hospital, Capital Medical University, No. 2 Anzhen Road, Chaoyang District, Beijing 100029, China. Email: leixu2001@hotmail.com.

Background: Computed tomography angiography-based global longitudinal strain (CTA-GLS) is feasible for myocardial assessment, but limited data are available for patients undergoing transcatheter aortic valve implantation (TAVI). This study sought to analyze the association between CTA-GLS and perioperative aortic regurgitation (AR), and its prognostic value in TAVI patients.

Methods: Consecutive TAVI recipients at Beijing Anzhen Hospital were enrolled in this retrospective study from June 2021 to January 2024. The patients underwent transthoracic echocardiography (TTE), and pre-TAVI CTA. Nonlinear relationships between CTA-GLS and AR were evaluated using restricted cubic splines (RCSs). The performance of the multivariate Cox proportional hazards models were assessed by the concordance index (C-index), integrated discrimination improvement (IDI), and net reclassification improvement (NRI).

Results: The study included 369 TAVI patients with a median age of 73.0 years, of whom 56.1% were male. CTA-GLS exhibited a strong nonlinear correlation with pre-procedural AR (P<0.001) and post-operative AR improvement (P=0.004). In the multivariate Cox proportional hazards regression, each 1% absolute decrease in CTA-GLS remained a significant predictor of all-cause mortality and heart failure hospitalization (HFH) post-TAVI [hazard ratio (HR): 1.47; 95% confidence interval (CI): 1.22–1.78; P<0.001]. The following three nested models were developed: Model 1, which included clinical parameters; Model 2, which included CTA-GLS, and Model 3, which combined both. Adding CTA-GLS improved the C-index from 0.66 (95% CI: 0.53–0.79) to 0.81 (95% CI: 0.75–0.87) (P=0.028), which was also reflected in the NRI [0.89 (95% CI: 0.56–1.22), P<0.001] and IDI [0.05 (95% CI: 0.02–0.09), P=0.003].

Conclusions: Pre-TAVI CTA-GLS is nonlinearly linked to pre-procedural AR and its improvement. It can be used to independently predict post-TAVI outcomes and adds incremental value to clinical parameters.

Keywords: Computed tomography angiography (CTA); global longitudinal strain (GLS); transcatheter aortic valve implantation (TAVI); aortic regurgitation (AR); prognosis

Submitted Apr 07, 2025. Accepted for publication Oct 15, 2025. Published online Nov 12, 2025.
doi: 10.21037/qims-2025-841
View this article at: https://dx.doi.org/10.21037/qims-2025-841

Introduction

Valvular heart disease is a major global health issue, affecting over 2% of the population (1). Transcatheter aortic valve implantation (TAVI) has become the recommended treatment for patients with severe symptomatic aortic stenosis (AS), yielding favorable results in terms of hemodynamics and clinical outcomes (2,3). This procedure is beneficial in managing pure aortic regurgitation (AR) and in younger, lower-risk patients with AS (4,5). While long-term outcomes and survival following TAVI are strongly associated with preoperative left ventricular (LV) function in patients with chronic AR (6,7), post-TAVI AR has been shown to significantly worsen clinical outcomes, leading to increased morbidity and mortality (8,9). Recent studies have highlighted that structural and functional cardiac alterations resulting from adverse cardiac remodeling are closely correlated with clinical prognosis (10-12). However, research on the relationship between AR, adverse LV remodeling, and long-term clinical outcomes is limited.

Echocardiography and strain imaging can provide advanced insights into the assessment of myocardial mechanics (13,14). However, LV ejection fraction (LVEF) can remain normal despite substantial myocardial damage (15). Global longitudinal strain (GLS) calculated using cardiac magnetic resonance (CMR) is a noninvasive imaging marker that detects subclinical myocardial deformation abnormalities before changes in LVEF occur and can predict adverse outcomes in patients undergoing TAVI (16,17). However, CMR is rarely used in patients with TAVI, and computed tomography angiography (CTA) is a prerequisite for patients for whom TAVI is being considered (18). CTA precisely measures the aortic valve anatomy and quantifies aortic valve calcification, enabling the accurate determination of TAVI prosthesis sizing and procedural access (19).

In a previous study, we established that CTA-GLS reliably evaluates changes in myocardial mechanics, yielding results comparable to those of CMR, and demonstrating good intra-observer agreement (20). Fukui *et al.* showed that CTA-GLS is a feasible and effective method and enhances risk stratification by offering independent and incremental prognostic value beyond clinical and echocardiographic parameters (21). CTA-GLS is clinically applicable and is also independently associated with outcomes after TAVI, even in patients with preserved LVEF (18,22). Thus, this study aimed to explore the potential interactions between CTA-GLS and perioperative AR, and to assess the prognostic value of CTA-GLS in patients undergoing TAVI. We present this article in accordance with the STROBE reporting checklist (available at https://qims.amegroups.com/article/view/10.21037/qims-2025-841/rc).

Methods

Study population

The study adhered to the principles of the Declaration of Helsinki and its subsequent amendments. The study protocol was approved by the Institutional Review Board (IRB) of Beijing Anzhen Hospital (No. 2025216X), which waived the requirement of informed consent due to the retrospective nature of this study.

Consecutive adult TAVI recipients at Beijing Anzhen Hospital were enrolled in this retrospective study from June 2021 to January 2024. Patients were included in the study if they met the following inclusion criteria: (I) had a diagnosis of severe symptomatic AS; and (II) were an appropriate candidate for TAVI. Patients were excluded from the study if they met any the following exclusion criteria: (I) had poor-quality images; (II) had incomplete LV coverage; and/or (III) were lost to follow-up.

The aortic valve morphology (including the bicuspid aortic valve morphology), prosthesis type (i.e., balloon-expandable valve, self-expanding valve, or AR valve) and size, access route, and the use of pre- and post-dilation procedures were recorded for all patients. The patients underwent comprehensive clinical evaluation, transthoracic echocardiography (TTE), and pre-TAVI CTA for planning. The clinical baseline characteristics included age, sex, body mass index (BMI), heart rate, brain natriuretic peptide (BNP) level, and New York Heart Association (NYHA) functional class. Information on each patient's prior history of smoking, drinking, chronic obstructive pulmonary disease, atrial fibrillation/flutter, coronary artery disease and revascularization, hypertension, hyperlipidemia, and diabetes mellitus was obtained from their medical records.

The clinical endpoints of this study were a composite of all-cause mortality and heart failure hospitalization (HFH) after TAVI. A hospitalization event qualified as an HFH event if it met the following pre-specified criteria based on objective evidence from medical records: (I) the presence of new or worsening signs and symptoms of heart failure (HF; e.g., dyspnea, orthopnea, pulmonary rales, or peripheral edema); and (II) the administration of intravenous diuretics and/or inotropic agents during hospitalization. Elevated natriuretic peptide levels at admission [BNP ≥400 pg/mL or N-terminal pro-B-type natriuretic peptide (NT-proBNP) ≥1,000 pg/mL] provided supportive—but not essential—evidence for adjudication. Follow-up was conducted via telephonic interviews or using medical records, and cardiac death events were classified according to Valve Academic Research Consortium-3 criteria (23). To ensure objectivity in the adjudication process, all potential events were evaluated by study reviewers who were blinded to treatment group assignments. The time to event for the composite outcome was defined as the interval from TAVI to the first adverse event. Patients who did not experience the composite endpoint event were censored at the date of their last known contact.

Echocardiographic parameters and definitions

The first TTE was performed preoperatively. The post-procedural evaluation was based on the first TTE obtained within one week of the TAVI. When multiple examinations were conducted during this period (including intraprocedural, 24–48-hour post-procedural, or pre-discharge assessments), the results from the initial TTE were consistently used. All patients completed TTE within this specified timeframe. The echocardiographic examinations followed standard clinical protocols, were performed by sonographers with varying qualifications, and employed a dual-reading and consensus process whereby each report was initially prepared by a junior physician, and then reviewed by an assessing physician who had access to the initial evaluation of the junior physician. The assessment clearly differentiated between paravalvular and transvalvular regurgitation, and all physicians involved in the reading process were unblinded to the patients' clinical information.

All the echocardiographic parameters were measured in accordance with current guidelines (24) and comprised LVEF, LV end-diastolic diameter (LVEDD), and tricuspid annular plane systolic excursion (TAPSE). The post-TAVI assessment of AR was performed according to the guidelines of the American Society of Echocardiography for assessing valvular regurgitation after percutaneous valve repair or replacement. This evaluation used color Doppler jet characteristics, continuous-wave and pulsed-wave Doppler techniques, and quantitative Doppler evaluation to determine the severity of AR.

All the patients' ultrasound assessments were evaluated by sonographers. Pre-procedural and post-procedural AR were graded using a five-class scheme as follows (23,25): 0, none or trace; 1, mild; 2, mild to moderate; 3, moderate; 4, moderate to severe; and 5, severe. The primary study endpoint was alterations in the AR class, with the AR of patients categorized as improved (AR grade decreased) or not improved (AR grade increased or unchanged). To align this scale with conventional grading categories and provide the quantitative criteria used for adjudication, a detailed mapping table has been included as Table S1.

CTA protocols and reconstruction

All the patients were examined using a dual-source computed tomography (CT) scanner (Somatom Definition Flash, Siemens Healthineers, Forchheim, Germany). The protocols and instrument parameters have been described in an earlier study (20). Prospective electrocardiogram gating was used for all scans without premedication for heart rate control, as patients with tachycardia (>100 beats per minute) or arrhythmias were referred for cardiology consultation. The improved temporal resolution of the CT systems maintained diagnostic image quality even at elevated heart rates. The scan range ran from 1.0 cm below the tracheal carina to 1.5 cm below the cardiac apex. Automated bolus tracking was performed with the region of interest positioned in the ascending aorta. Contrast agent (Iohexol 350, GE Ltd., WI, USA) was administered at 0.8 mL/kg with a flow rate of 4.0–5.0 mL/s, followed by a 30 mL saline flush. The CTA cine series was reconstructed for conventional function and strain analysis. This reconstruction used a slice thickness of 0.6 mm with an increment of 0.4 mm. The images were reconstructed in 11 phases per cardiac cycle, at 10% intervals spanning 0% to 100% of the R-R interval. An iterative reconstruction factor of three was applied during this process. The volume CT dose index was 22.48±8.06 mGy, and the dose-length product was 782.88±199.04 mGy·cm. The effective radiation dose from the CT scans was calculated using the dose-length product multiplied by an older conversion factor of 0.014 $mSv\cdot mGy^{-1}\cdot cm^{-1}$ (25).

CTA-GLS measurement

The CTA datasets were imported into the commercially available CVI software (version 5.17, Circle Cardiovascular Imaging Inc., Calgary, AB, Canada). For the strain analysis, two-dimensional cine loops of both two- and four-chamber views, along with a sequence of short-axis views (comprising 10–14 slices from the basal to the apical left ventricle), were created. The CVI software was used for this purpose, with each slice having a thickness of 8 mm and no increment. For the strain analysis, the end-systolic and end-diastolic cardiac phases were automatically identified. Three long-axis views (four-, three-, and two-chamber) were reconstructed using double-oblique multiplanar reconstructions. Subsequently, the endocardial border was manually outlined in each view at end-diastole (when the LV cavity was the largest) and end-systole (when the LV cavity was the smallest). Care was taken to avoid placing points at the mitral annulus, LV outflow tract areas, and papillary muscles. This process was followed by automated feature-tracking (FT) propagation throughout the cardiac cycle and a review of the individual tracings. Manual adjustments of the segmented contours were performed at key cardiac phases (end-systole and end-diastole) as necessary to optimize tracking accuracy and ensure proper alignment with myocardial motion. The cine loops were then imported into the FT model of the software. The CTA-GLS was then derived from the strain curves. Research has shown that CTA-GLS offers reliable and interchangeable results for assessing myocardial mechanical changes compared to CMR, with good intra-observer agreement (20). LV function and strain were assessed by two reporting clinicians: Y.C.C. (with 4 years of experience), and Y.F.G. (with 5 years of experience). A subset of 50 patients from the study cohort was randomly selected to examine inter-observer agreement based on the intraclass correlation coefficient (ICC). In this study, a reduction in its absolute value of CTA-GLS (i.e., less negative values) reflected worse LV systolic function.

Statistical analysis

The statistical analysis was performed using R software (version 4.4.1; R Foundation for Statistical Computing, Vienna, Austria). The continuous variables are expressed as the mean ± standard deviation, and the categorical variables are reported as the frequency or percentage. The Kolmogorov-Smirnov test was used to assess the normality of the continuous data. Group differences were analyzed using the independent *t*-test for the normally distributed data and the Mann-Whitney *U*-test for the non-normally distributed data. Pearson's Chi-squared test was used to analyze the categorical variables. The nonlinear relationship between CTA-GLS and pre-procedural AR, post-operative AR improvement, and post-procedural AR was evaluated using restricted cubic splines (RCSs). Multiple imputation was applied to manage missing data. Multivariate Cox proportional hazards models were developed. Univariate regression models were initially established for each variable and those with P values <0.100 in the univariate analysis were included in multivariate regression. A backward-selection approach was used to develop the multivariate models, and variables with P values <0.05 were retained. Estimated hazard ratios (HRs) were reported together with their 95% confidence intervals (CIs) and P values. The "self-expanding valve" and "aortic regurgitation valve" categories were combined into a single group due to low sample sizes. The "balloon-expandable valve" group was used as the reference group. Firth's penalized-likelihood regression was employed to address potential small-sample bias due to the low number of events in our cohort. This method corrects for bias in maximum likelihood estimation by modifying the likelihood function (26). To assess the robustness of the primary study findings, a complete-case sensitivity analysis was also performed. A clinical model was constructed with variables found to be significant univariate predictors of the events, which was subsequently integrated with CTA-GLS to form a nested model. Sensitivity analyses were conducted to compare different models. The sensitivity, specificity, positive predictive value (PPV), and negative predictive value (NPV) were reported, along with the 95% CIs. Models were assessed in terms of discrimination and calibration using the concordance index (C-index) and the Akaike information criterion (AIC), respectively. A time-dependent receiver operating characteristic curve at each time quartile point was also calculated to assess the predictive value of the Cox proportional hazards models. In addition, integrated discrimination improvement (IDI) and net reclassification improvement (NRI) were applied to quantify the performance enhancement of the CTA-GLS combined model relative to the clinical model. Kaplan-Meier survival curves were used for the survival analysis.

Results

Study population

Figure 1 presents the patient screening and selection process. A total of 457 consecutive patients successfully underwent TAVI at Beijing Anzhen Hospital from June 2021 to January 2024 and met the study inclusion criteria. Of these, 16 patients with poor-quality pre-TAVI CTA images for strain analysis due to breathing or arrhythmia artifacts, 33 patients with incomplete LV coverage, and 39 patients who were lost to follow-up (36 could not be

457 consecutive patients underwent TAVI at Beijing Anzhen Hospital between June 2021 and January 2024

→ Excluded patients (n=88)
- Poor image quality (n=16)
- Incomplete LV coverage (n=33)
- Lost to follow-up (n=39)

369 pre-TAVI CTA images were eligible for CTA-GLS and prognostic analysis

Events n=23 | No events n=346

Figure 1 Study flowchart. CTA, computed tomography angiography; CTA-GLS, computed tomography angiography-based global longitudinal strain; LV, left ventricular; TAVI, transcatheter aortic valve implantation.

contacted despite multiple attempts, and 3 refused to cooperate further) were excluded from the study. The date of last contact was August 23, 2024, yielding a complete follow-up rate of 89.1% (369 of 414). Thus, ultimately, 369 patients [median age: 73.0 years, interquartile range (IQR), 68–78 years; males: 56.1%] were included in the study.

The indication for TAVI was AS in 65.0% (240 of 369) of the patients, mixed disease in 21.1% (78 of 369), and regurgitation in 13.8% (51 of 369). All procedures were performed via transfemoral access. Events occurred in 6.2% (23 of 369) of the patients over 486 days (IQR, 322–751 days) of follow-up. All-cause mortality was the primary driver (n=19), with only four adjudicated HFH events recorded. *Table 1* summarizes the baseline characteristics of the patients, and provides comparisons between those who experienced events after TAVI and those who did not during the follow-up period. The inter-reader agreement ICC was 0.91 for the measurement of CTA-GLS. A higher prevalence of smoking and CTA-GLS and lower heart rate were observed in the events group compared with the no-events group (all P<0.05). No differences were found between the two groups in terms of the other clinical risk factors, previous history, and echocardiographic parameters, as well as key procedural characteristics, including prosthesis type and size, and the use of pre-dilation or post-dilation procedures (all P>0.05). A comparison of the key baseline characteristics between the patients included in the final analysis (n=369) and those excluded solely due to loss to follow-up (n=39) revealed no statistically significant differences (Table S2).

Association among pre-procedural AR, post-operative AR improvement, post-procedural AR, and CTA-GLS

A Sankey plot (Figure S1) was generated to depict the percentage changes in the AR class from baseline to post-TAVI. At baseline, 47 patients (12.7%) were categorized as class 0, 156 (42.3%) as class 1, 5 (1.4%) as class 2, 68 (18.4%) as class 3, 16 (4.3%) as class 4, and 77 (20.9%) as class 5. The Sankey plot showed the proportions of each AR grade from baseline to post-TAVI. In the paired analysis, 239 of 369 (64.8%) patients experienced AR improvement of at least 1 grade after TAVI in their post-operative echocardiography compared with their preoperative echocardiography. Conversely, 130 of 369 (35.2%) patients exhibited an unchanged or increased AR grade immediately after TAVI.

RCS functions relating to pre-procedural AR, post-operative AR improvement, post-procedural AR, and CTA-GLS are illustrated in *Figure 2*. CTA-GLS was strongly nonlinearly correlated with pre-procedural AR (P for nonlinear <0.001) and post-operative AR improvement (P for nonlinear =0.004). The RCS analysis revealed an "inverted U-shaped" association between CTA-GLS and pre-procedural AR, showing an initially increasing and then decreasing trend with a cutoff value of −9.7%. The RCS curve demonstrated that CTA-GLS led to a reduced event rate of AR improvement with a reduced magnitude of CTA-GLS. There was no evidence of a nonlinear trend between CTA-GLS and post-procedural AR (P for nonlinear =0.174).

Table 1 Baseline characteristics

Characteristic	All (n=369)	Events (n=23)	No events (n=346)	P value
Age, years	73.0 (68.0, 78.0)	74.0 (69.0, 81.0)	73 (68.0, 79.0)	0.355
Sex (male)	207 (56.1)	17 (73.9)	190 (54.9)	0.075
Follow-up period, days	486.0 (322.0, 751.0)	651.0 (456.0, 871.5)	475.0 (315.3, 747.3)	0.033
BMI, kg/m^2	24.2 (22.1, 26.7)	24.5 (22.7, 28.1)	24.2 (22.1, 26.7)	0.543
Heart rate, bmp	72.0 (68.0, 80.0)	69.0 (60.5, 72.5)	72.5 (68.0, 80.0)	0.008
Diabetes	100 (27.1)	4 (17.4)	96 (27.7)	0.279
Hypertension	227 (61.5)	18 (78.3)	209 (60.4)	0.088
Smoking	83 (22.5)	9 (39.1)	74 (21.4)	0.048
Alcohol	50 (13.6)	3 (13.0)	47 (13.6)	>0.999
Dyslipidemia	180 (48.8)	10 (43.5)	170 (49.1)	0.599
BNP, pg/mL	851.0 (289.0, 2,249.0)	1,085.0 (504.0, 2,251.0)	842.0 (275.3, 2,248.8)	0.129
NYHA functional class III or IV	168 (45.5)	14 (60.9)	154 (44.5)	0.127
COPD	17 (4.6)	2 (8.7)	15 (4.3)	0.287
AF	40 (10.8)	3 (13.0)	37 (10.7)	0.727
CAD	206 (55.8)	13 (56.5)	193 (55.8)	0.945
Previous PCI	54 (14.6)	4 (17.4)	50 (14.5)	0.759
Previous CABG	3 (0.8)	1 (4.3)	2 (0.6)	0.176
LVEF, %	60.0 (53.0, 66.0)	58.0 (52.0, 61.5)	60.0 (53.0, 66.0)	0.167
LVEDD, mm	50.0 (45.0, 58.0)	50.0 (44.0, 57.0)	50.0 (46.0, 58.0)	0.801
TAPSE, mm	20.6 (19.0, 22.6)	19.6 (19.0, 22.3)	20.6 (19.0, 22.6)	0.363
Moderate to severe AR class (class 3–5)	161 (43.6)	149 (43.1)	12 (52.2)	0.394
CTA-GLS, %	–8.9 (–12.1, –6.6)	–6.0 (–7.4, –5.2)	–9.2 (–12.3, –6.7)	<0.001
Bicuspid valve	43 (11.7)	4 (17.4)	39 (11.3)	0.326
Prothesis size, mm	20.0 (18.0, 22.0)	22.0 (19.0, 22.0)	20.0 (18.0, 22.0)	0.039
Prothesis type				0.297
Balloon-expandable valve	346 (93.8)	21 (91.3)	325 (93.9)	
Self-expanding valve	9 (2.4)	0 (0.0)	9 (2.6)	
Aortic regurgitation valve	14 (3.8)	2 (8.7)	12 (3.5)	
Pre-dilation procedure	287 (77.8)	21 (91.3)	266 (76.9)	0.107
Post-dilation procedure	142 (38.5)	8 (34.8)	134 (38.7)	0.706

Values are presented as median (interquartile range) or number (percentage). AF, atrial fibrillation; AR, aortic regurgitation; BMI, body mass index; BNP, brain natriuretic peptide; CABG, coronary artery bypass grafting; CAD, coronary artery disease; COPD, chronic obstructive pulmonary disease; CTA-GLS, computed tomography angiography-based global longitudinal strain; LVEDD, left ventricular end-diastolic diameter; LVEF, left ventricular ejection fractions; NYHA, New York Heart Association; PCI, percutaneous coronary intervention; TAPSE, tricuspid annular plane systolic excursion.

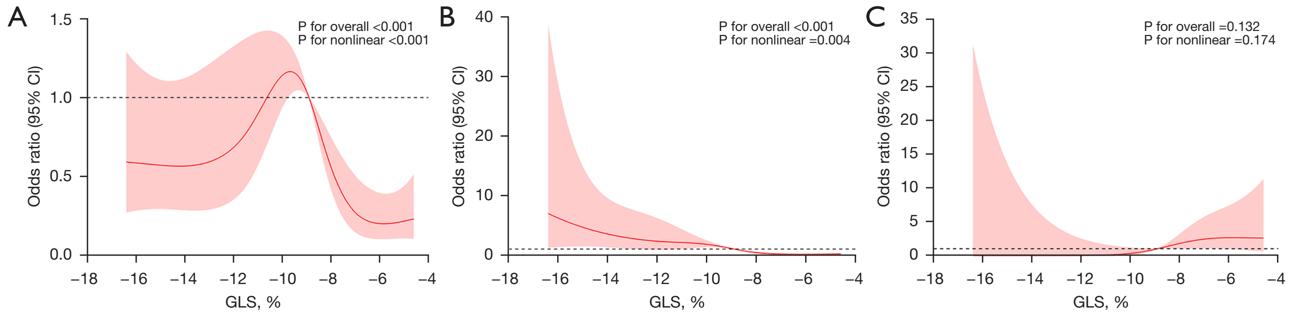

Figure 2 The RCS analysis of associations between CTA-GLS and pre-procedural AR, post-operative AR improvement, and postprocedural AR. The RCS analysis revealed an "inverted U-shaped" association between CTA-GLS and pre-procedural AR (A). The inflection point of the RCS curve was identified at CTA-GLS as −9.7%. The RCS analysis suggested an "L-shaped" association between CTA-GLS and post-operative AR improvement (B). The inflection point of the RCS curve was identified at CTA-GLS as −10.3%. There was no nonlinear relationship between CTA-GLS and post-procedural AR (C). More negative values on the X-axis indicate better left ventricular function. AR, aortic regurgitation; CI, confidence interval; CTA-GLS, computed tomography angiography-based global longitudinal strain; GLS, global longitudinal strain; RCS, restricted cubic spline.

Prognosis

The results of the Cox proportional hazards regression are presented in *Table 2*. In the univariate Cox regression analysis, sex (HR =2.54; 95% CI: 1.00–6.45), smoking (HR =2.89; 95% CI: 1.24–6.73), NYHA functional class III or IV (HR =2.18; 95% CI: 0.94–5.06), and CTA-GLS (HR =1.48; 95% CI: 1.24–1.78) were significant predictors of all-cause mortality and HFH after TAVI (all P<0.100). Only CTA-GLS (HR =1.47; 95% CI: 1.22–1.78) remained in the Cox proportional hazards regression (P<0.001). In Firth's penalized-likelihood regression analysis (Table S3), CTA-GLS remained significantly associated with the outcome (HR =1.45, 95% CI: 1.22–1.77, P<0.001). In the Kaplan-Meier survival analysis, there was an increased risk for the composite outcome endpoint according to the presence of a reduced magnitude of CTA-GLS (*Figure 3*). Only two variables had missing values: 31 of 369 (8.4%) for TAPSE, and 78 of 369 (21.1%) for prosthesis size. A sensitivity Cox regression analysis (Table S4) was performed on the 265 patients with complete data. The results of this analysis were entirely consistent with the primary model, demonstrating that CTA-GLS remained significantly associated with the outcome (HR =1.68, 95% CI: 1.22–2.32, P=0.001).

To assess the incremental value of CTA-GLS in predicting post-TAVI AR improvement, the following three nested models were constructed: Model 1, which included the clinical parameters remaining in the univariate Cox regression analysis; Model 2, which included the CTA-GLS parameter; and Model 3, which comprised Model 1 + Model 2. The corresponding accuracies, sensitivities, specificities, PPVs, and NPVs of each model are set out in Table S5. Model 1, Model 2, and Model 3 exhibited sensitivities of 0.65, 0.83, and 0.96, and specificities of 0.65, 0.65, and 0.56, respectively. Compared with Model 1, Model 3 showed significantly higher sensitivity, specificity, and NPV (all P<0.001). However, no significant differences were observed in the sensitivities, PPVs, and NPVs between Model 2 and Model 3 (all P>0.05). The addition of CTA-GLS improved model fit and model performance (*Table 3*). Integrating CTA-GLS into Model 1 significantly increased the C-index from 0.66 (95% CI: 0.53–0.79) to 0.81 (95% CI: 0.75–0.87) (P=0.028). This enhancement was also reflected in the NRI [0.89 (95% CI: 0.56–1.22), P<0.001] and IDI [0.05 (95% CI: 0.02–0.09), P=0.003].

Discussion

This study demonstrated three main findings. First, a nonlinear relationship was observed between pre-procedural AR and CTA-GLS, as well as between post-operative AR improvement and CTA-GLS. Second, a comprehensive assessment of long-term outcomes in patients undergoing TAVI is feasible using CTA-GLS. Third, CTA-GLS could potentially serve as an adjunctive tool for assessing TAVI patients; however, further studies need to be conducted to determine its role relative to current guideline-recommended protocols.

Table 2 Univariate and multivariate analysis of clinical outcomes

Characteristic	Univariate		Multivariate	
	HR (95% CI)	P value	HR (95% CI)	P value
Age, years	1.02 (0.96, 1.07)	0.567		
Sex (male)	2.54 (1.00, 6.45)	0.050	1.36 (0.46, 4.03)	0.576
BMI	1.06 (0.94, 1.20)	0.319		
Heart rate	0.96 (0.92, 1.01)	0.127		
Diabetes	0.66 (0.22, 1.97)	0.460		
Hypertension	1.76 (0.65, 4.76)	0.262		
Smoking	2.89 (1.24, 6.73)	0.014	2.45 (0.90, 6.67)	0.081
Alcohol	1.03 (0.31, 3.49)	0.958		
Dyslipidemia	0.92 (0.40, 2.10)	0.837		
BNP	1.00 (1.00, 1.00)	0.786		
NYHA functional class III or IV	2.18 (0.94, 5.06)	0.069	1.87 (0.80, 4.41)	0.151
Moderate to severe AR class (class 3–5)	1.49 (0.66, 3.39)	0.339		
COPD	2.46 (0.57, 10.61)	0.226		
AF	1.50 (0.44, 5.13)	0.520		
CAD	1.26 (0.55, 2.90)	0.581		
Previous PCI	1.26 (0.43, 3.73)	0.677		
Previous CABG	3.05 (0.40, 23.15)	0.281		
LVEF	0.99 (0.95, 1.03)	0.579		
LVEDD	1.00 (0.95, 1.05)	0.873		
TAPSE	0.98 (0.86, 1.11)	0.753		
CTA-GLS	1.48 (1.24, 1.78)	<0.001	1.47 (1.22, 1.78)	<0.001
Bicuspid valve	1.21 (0.41, 3.59)	0.732		
Prothesis size	1.14 (0.91, 1.44)	0.249		
Prothesis type	2.78 (0.35, 22.08)	0.333		
Pre-dilation procedure	1.97 (0.46, 8.45)	0.360		
Post-dilation procedure	1.22 (0.51, 2.90)	0.652		

AF, atrial fibrillation; AR, aortic regurgitation; BMI, body mass index; BNP, brain natriuretic peptide; CABG, coronary artery bypass grafting; CAD, coronary artery disease; CI, confidence interval; COPD, chronic obstructive pulmonary disease; CTA-GLS, computed tomography angiography-based global longitudinal strain; HR, hazard ratio; LVEDD, left ventricular end-diastolic diameter; LVEF, left ventricular ejection fractions; NYHA, New York Heart Association; PCI, percutaneous coronary intervention; TAPSE, tricuspid annular plane systolic excursion.

TAVI is increasingly being used to treat predominant AR, degenerated bioprosthetic valves, and bicuspid aortic valves in selected cases (27). However, severe AR pre-TAVI and post-TAVI AR have been reported to be associated with increased long-term mortality (28,29). Pre-existing AR results in volume overload, which leads to LV dilatation and eccentric hypertrophy (30). Despite variations in baseline AR class at the time of the TAVI procedure, patients have been reported to exhibit dynamic improvements in cardiac remodeling, which could be due to the relief from pressure and volume overload (31). Therefore, myocardial change and function were assessed using GLS to detect early myocardial changes during therapy (32). The results of this assessment indicated that cardiac remodeling was associated with pre-procedural AR and post-operative AR improvement. The RCS analysis revealed an "inverted U-shaped" association between CTA-GLS and pre-procedural AR. Specifically, as the magnitude of CTA-GLS decreased, there was an initial increase in the severity of AR up to a cutoff value of −9.7%, after which further decreases in magnitude of CTA-GLS were associated with a decrease in AR severity. This pattern suggests a complex interplay that may be explained by compensatory mechanisms rather than a straightforward causal relationship. The present study suggests that higher GLS is associated with diminished myocardial contractility and reduced LV functional reserve, which may compromise the ability of the heart to adapt to the hemodynamic changes after TAVI. This observation might be related to several factors, such as the potential contribution of HF to ventricular dysfunction or technical considerations in AR assessment. These preliminary findings suggest a need for further exploration of valvular-ventricular interactions in severe AS.

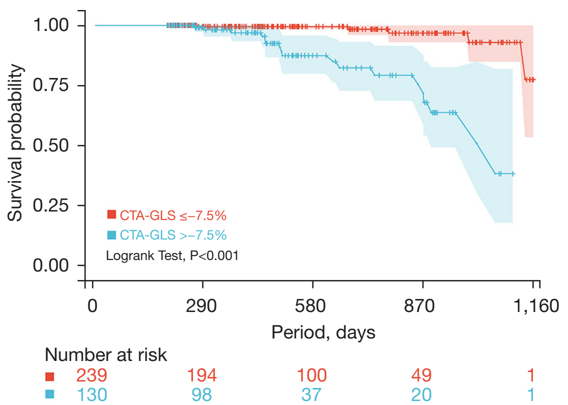

Figure 3 Kaplan-Meier curves for composite outcomes. Survival curves by change in CTA-GLS. Patients with baseline CTA-GLS >−7.5% had a higher risk of the composite outcome of death or heart failure hospitalization than those with baseline CTA-GLS ≤−7.5% (P<0.001). More negative values on the X-axis indicate better left ventricular function. CTA-GLS, computed tomography angiography-based global longitudinal strain.

The inter-observer agreement for CTA-GLS measurements was excellent. Therefore, myocardial strain assessment appears promising for further risk stratification in patients before TAVI. This evaluation is essential to guide subsequent interventions, such as post-dilation procedures, valve-in-valve procedures, or leak closure, to optimize patient outcomes. No correlation was found between CTA-GLS and post-procedural AR. This might be because the rates of moderate to severe AR after TAVR depend on the sizing of the prosthesis and the anatomical structure of the aortic root, the imaging modalities employed, and the timing of the assessment, as well as the procedure (33). Further, it should be recognized that immediate post-procedural AR is predominantly influenced by device-related, anatomical, and procedural factors, including the prosthesis type/size, degree and pattern of annular/LV outflow tract (LVOT) calcification, implantation depth, and use of post-dilatation procedures. These factors likely determine the severity of early post-TAVR AR, which may help explain the lack of correlation between CTA-GLS and post-procedural AR observed in this study.

Poor pre-procedural GLS has been reported to be significantly correlated with adverse clinical outcomes post-TAVI (13,14). LV geometric deformation before

Table 3 Incremental prognostic value of CTA-GLS

Model-fit statistics	Model 1	Model 2	Model 3
AIC	207	190	188
Model performance (95% CI)			
C-index	0.66 (0.53, 0.79)	0.77 (0.67, 0.86)	0.81 (0.75, 0.87)
AUC (*t*) at *t*=322 days	0.71 (0.61, 0.81)	0.60 (0.50, 0.70)	0.70 (0.65, 0.76)
AUC (*t*) at *t*=486 days	0.56 (0.45, 0.67)	0.82 (0.75, 0.89)	0.83 (0.79, 0.87)
AUC (*t*) at *t*=751 days	0.69 (0.62, 0.77)	0.83 (0.78, 0.88)	0.87 (0.83, 0.91)

Model 1: sex, smoking, age, and NYHA functional class III or IV; Model 2: CTA-GLS; Model 3: Model 1 + Model 2. AIC, Akaike's an information criterion; AUC, are under the curve; CI, confidence interval; C-index, concordance index; CTA-GLS, computed tomography angiography-based global longitudinal strain; NYHA, New York Heart Association.

TAVI may play a critical role in influencing patient prognosis after the procedure (34). While TTE remains the primary modality for assessing myocardial function in TAVI patients, CTA-GLS may serve as an adjunctive tool in select cases, particularly when additional functional data are needed beyond standard imaging. According to Koike *et al.*, myocardial evaluation with CTA using CT-based extracellular volume and CTA-GLS is feasible and is independently associated with 1-year outcomes after TAVI, even in those with preserved LVEF (18). The current study further demonstrated that pre-procedural CTA-GLS serves as a valuable predictor of events after TAVI. Importantly, CTA-GLS provides additional predictive value beyond conventional clinical and echocardiographic assessments of death or HFH. The present study is the first to show the nonlinear relationship between pre-procedural AR, post-TAVI AR improvement, and CTA-GLS.

This finding highlights the potential of CTA-GLS as a comprehensive and effective tool in assessing and managing patients undergoing TAVI procedures. Indeed, CTA-GLS holds immense potential in clinical practice beyond predicting improvement in post-TAVI AR and long-term outcomes. It could not only assist clinicians to identify patients who are likely to derive greater benefits from the operation but could also improve risk stratification and refine the timing of the intervention. From an implementation perspective, CTA-GLS could be integrated into routine pre-TAVI planning CT with minimal additional workflow when software solutions are available. However, the broader adoption of this approach still requires addressing key challenges, including the external validation and standardization of FT protocols. In summary, incorporating CTA-GLS into clinical practice will enhance the precision of patient management throughout the TAVI process. Further, as CTA is a part of the work-up for TAVI, the CTA-GLS assessment can be easily added to standard TAVI CT planning. However, the imaging parameter needs to be integrated into future clinical trials to determine whether it can be potentially used for decision-making, including decisions related to the timing of the intervention and post-TAVR follow-up.

This study had several limitations. First, this was a retrospective study; thus, the findings need to be verified in prospective studies. The exact shape of the RCS curve between pre-procedural CTA-GLS and post-TAVI AR improvement needs to be clarified. Second, an accurate assessment of AR class could be challenging when severe AS or mixed aortic valve disease is present. Although echocardiographic analyses were not performed under core laboratory supervision, they were conducted by highly experienced specialists and were clinically relevant. Future studies incorporating advanced imaging modalities like four-dimensional flow magnetic resonance imaging or intraprocedural hemodynamic assessment could help better characterize AR severity in this challenging population. Third, the effect of the presence of bicuspid aortic valves and the effect of prosthesis-patient mismatch after TAVI was not assessed. The absence of systematically collected device-related, anatomical, and procedural covariates (e.g., the valve model, implantation depth, and calcification distribution) might have confounded the post-TAVI analysis. Further, the generalizability of our findings might be limited by the single-center retrospective design and the relatively low event rate observed in this cohort. Despite the relatively low event rate (6%) of our study, sensitivity analyses using Firth's bias-reduced logistic regression confirmed our primary findings. However, the generalizability of these results to populations with different event rates warrants further investigation.

Conclusions

CTA-GLS can be used to evaluate perioperative AR and prognosis in TAVI patients, and is independently associated with all-cause mortality and HFH. The integration of CTA-GLS into the clinical assessment provides valuable information beyond clinical parameters, which demonstrates its potential as an effective imaging tool to enhance risk stratification and treatment response. However, more prospective studies are required to validate these findings.

Acknowledgments

None.

Footnote

Reporting Checklist: The authors have completed the STROBE reporting checklist. Available at https://qims.amegroups.com/article/view/10.21037/qims-2025-841/rc

Data Sharing Statement: Available at https://qims.amegroups.com/article/view/10.21037/qims-2025-841/dss

Funding: This study was supported by grants from the National Key R&D Program of China (No.

2022YFE0209800), the National Natural Science Foundation of China (Nos. 82271986 and U1908211), and the Beijing Anzhen Hospital High-level Research Funding (No. 2024AZC2002).

Conflicts of Interest: All authors have completed the ICMJE uniform disclosure form (available at https://qims.amegroups.com/article/view/10.21037/qims-2025-841/coif). L.X. reports this study was supported by the National Key R&D Program of China (No. 2022YFE0209800), the National Natural Science Foundation of China (Nos. 82271986 and U1908211), and the Beijing Anzhen Hospital High-level Research Funding (No. 2024AZC2002). The other authors have no conflicts of interest to declare.

Ethical Statement: The authors are accountable for all aspects of the work in ensuring that questions related to the accuracy or integrity of any part of the work are appropriately investigated and resolved. The investigation adhered to the principles of the Declaration of Helsinki and its subsequent amendments. The study protocol was approved by the Institutional Review Board (IRB) of Beijing Anzhen Hospital (No. 2025216X). The requirement for informed consent was waived by the IRB due to the retrospective nature of this study.

References

1. Nkomo VT, Gardin JM, Skelton TN, Gottdiener JS, Scott CG, Enriquez-Sarano M. Burden of valvular heart diseases: a population-based study. Lancet 2006;368:1005-11.
2. Otto CM, Nishimura RA, Bonow RO, Carabello BA, Erwin JP 3rd, Gentile F, Jneid H, Krieger EV, Mack M, McLeod C, O'Gara PT, Rigolin VH, Sundt TM 3rd, Thompson A, Toly C. 2020 ACC/AHA Guideline for the Management of Patients With Valvular Heart Disease: A Report of the American College of Cardiology/American Heart Association Joint Committee on Clinical Practice Guidelines. Circulation 2021;143:e72-e227.
3. Vahanian A, Beyersdorf F, Praz F, Milojevic M, Baldus S, Bauersachs J, et al. 2021 ESC/EACTS Guidelines for the management of valvular heart disease. Eur Heart J 2022;43:561-632. Erratum in: Eur Heart J 2022;43:2022.
4. Sawaya FJ, Deutsch MA, Seiffert M, Yoon SH, Codner P, Wickramarachchi U, et al. Safety and Efficacy of Transcatheter Aortic Valve Replacement in the Treatment of Pure Aortic Regurgitation in Native Valves and Failing Surgical Bioprostheses: Results From an International Registry Study. JACC Cardiovasc Interv 2017;10:1048-56.
5. Rawasia WF, Khan MS, Usman MS, Siddiqi TJ, Mujeeb FA, Chundrigar M, Kalra A, Alkhouli M, Kavinsky CJ, Bhatt DL. Safety and efficacy of transcatheter aortic valve replacement for native aortic valve regurgitation: A systematic review and meta-analysis. Catheter Cardiovasc Interv 2019;93:345-53.
6. Hira RS, Vemulapalli S, Li Z, McCabe JM, Rumsfeld JS, Kapadia SR, Alam M, Jneid H, Don C, Reisman M, Virani SS, Kleiman NS. Trends and Outcomes of Off-label Use of Transcatheter Aortic Valve Replacement: Insights From the NCDR STS/ACC TVT Registry. JAMA Cardiol 2017;2:846-54.
7. Santos-Martínez S, Amat-Santos IJ. New Challenging Scenarios in Transcatheter Aortic Valve Implantation: Valve-in-valve, Bicuspid and Native Aortic Regurgitation. Eur Cardiol 2021;16:e29.
8. Van Belle E, Juthier F, Susen S, Vincentelli A, Iung B, Dallongeville J, et al. Postprocedural aortic regurgitation in balloon-expandable and self-expandable transcatheter aortic valve replacement procedures: analysis of predictors and impact on long-term mortality: insights from the FRANCE2 Registry. Circulation 2014;129:1415-27.
9. Sinning JM, Vasa-Nicotera M, Chin D, Hammerstingl C, Ghanem A, Bence J, Kovac J, Grube E, Nickenig G, Werner N. Evaluation and management of paravalvular aortic regurgitation after transcatheter aortic valve replacement. J Am Coll Cardiol 2013;62:11-20.
10. Ajmone Marsan N, Delgado V, Shah DJ, Pellikka P, Bax JJ, Treibel T, Cavalcante JL. Valvular heart disease: shifting the focus to the myocardium. Eur Heart J 2023;44:28-40.
11. Généreux P, Pibarot P, Redfors B, Mack MJ, Makkar RR, Jaber WA, et al. Staging classification of aortic stenosis based on the extent of cardiac damage. Eur Heart J 2017;38:3351-8.
12. Fukui M, Gupta A, Abdelkarim I, Sharbaugh MS, Althouse AD, Elzomor H, Mulukutla S, Lee JS, Schindler JT, Gleason TG, Cavalcante JL. Association of Structural and

Functional Cardiac Changes With Transcatheter Aortic Valve Replacement Outcomes in Patients With Aortic Stenosis. JAMA Cardiol 2019;4:215-22.
13. Meucci MC, Butcher SC, Galloo X, van der Velde ET, Marsan NA, Bax JJ, Delgado V. Noninvasive Left Ventricular Myocardial Work in Patients with Chronic Aortic Regurgitation and Preserved Left Ventricular Ejection Fraction. J Am Soc Echocardiogr 2022;35:703-711.e3.
14. Yang LT, Michelena HI, Scott CG, Enriquez-Sarano M, Pislaru SV, Schaff HV, Pellikka PA. Outcomes in Chronic Hemodynamically Significant Aortic Regurgitation and Limitations of Current Guidelines. J Am Coll Cardiol 2019;73:1741-52.
15. Grigioni F, Clavel MA, Vanoverschelde JL, Tribouilloy C, Pizarro R, Huebner M, et al. The MIDA Mortality Risk Score: development and external validation of a prognostic model for early and late death in degenerative mitral regurgitation. Eur Heart J 2018;39:1281-91.
16. Alashi A, Mentias A, Abdallah A, Feng K, Gillinov AM, Rodriguez LL, Johnston DR, Svensson LG, Popovic ZB, Griffin BP, Desai MY. Incremental Prognostic Utility of Left Ventricular Global Longitudinal Strain in Asymptomatic Patients With Significant Chronic Aortic Regurgitation and Preserved Left Ventricular Ejection Fraction. JACC Cardiovasc Imaging 2018;11:673-82.
17. Fukui M, Thoma F, Sultan I, Mulukutla S, Elzomor H, Lee JS, Schindler JT, Gleason TG, Cavalcante JL. Baseline Global Longitudinal Strain Is Associated With All-Cause Mortality After Transcatheter Aortic Valve Replacement. JACC Cardiovasc Imaging 2020;13:1092-4.
18. Koike H, Fukui M, Treibel T, Stanberry LI, Cheng VY, Enriquez-Sarano M, Schmidt S, Schelbert EB, Wang C, Okada A, Phichaphop A, Sorajja P, Bapat VN, Leipsic J, Lesser JR, Cavalcante JL. Comprehensive Myocardial Assessment by Computed Tomography: Impact on Short-Term Outcomes After Transcatheter Aortic Valve Replacement. JACC Cardiovasc Imaging 2024;17:396-407.
19. Blanke P, Weir-McCall JR, Achenbach S, Delgado V, Hausleiter J, Jilaihawi H, Marwan M, Norgaard BL, Piazza N, Schoenhagen P, Leipsic JA. Computed tomography imaging in the context of transcatheter aortic valve implantation (TAVI) / transcatheter aortic valve replacement (TAVR): An expert consensus document of the Society of Cardiovascular Computed Tomography. J Cardiovasc Comput Tomogr 2019;13:1-20.
20. Wang R, Fang Z, Wang H, Schoepf UJ, Emrich T, Giovagnoli D, Biles E, Zhou Z, Du Z, Liu T, Xu L. Quantitative analysis of three-dimensional left ventricular global strain using coronary computed tomography angiography in patients with heart failure: Comparison with 3T cardiac MR. Eur J Radiol 2021;135:109485.
21. Fukui M, Hashimoto G, Lopes BBC, Stanberry LI, Garcia S, Gössl M, Enriquez-Sarano M, Bapat VN, Sorajja P, Lesser JR, Cavalcante JL. Association of baseline and change in global longitudinal strain by computed tomography with post-transcatheter aortic valve replacement outcomes. Eur Heart J Cardiovasc Imaging 2022;23:476-84.
22. Gegenava T, van der Bijl P, Vollema EM, van der Kley F, de Weger A, Hautemann D, Reiber JHC, Ajmone Marsan N, Bax JJ, Delgado V. Prognostic Influence of Feature Tracking Multidetector Row Computed Tomography-Derived Left Ventricular Global Longitudinal Strain in Patients with Aortic Stenosis Treated With Transcatheter Aortic Valve Implantation. Am J Cardiol 2020;125:948-55.
23. Généreux P, Piazza N, Alu MC, Nazif T, Hahn RT, et al. Valve Academic Research Consortium 3: Updated Endpoint Definitions for Aortic Valve Clinical Research. J Am Coll Cardiol 2021;77:2717-46.
24. Zoghbi WA, Asch FM, Bruce C, Gillam LD, Grayburn PA, Hahn RT, Inglessis I, Islam AM, Lerakis S, Little SH, Siegel RJ, Skubas N, Slesnick TC, Stewart WJ, Thavendiranathan P, Weissman NJ, Yasukochi S, Zimmerman KG. Guidelines for the Evaluation of Valvular Regurgitation After Percutaneous Valve Repair or Replacement: A Report from the American Society of Echocardiography Developed in Collaboration with the Society for Cardiovascular Angiography and Interventions, Japanese Society of Echocardiography, and Society for Cardiovascular Magnetic Resonance. J Am Soc Echocardiogr 2019;32:431-75.
25. Pibarot P, Hahn RT, Weissman NJ, Arsenault M, Beaudoin J, Bernier M, et al. Association of Paravalvular Regurgitation With 1-Year Outcomes After Transcatheter Aortic Valve Replacement With the SAPIEN 3 Valve. JAMA Cardiol 2017;2:1208-16.
26. Heinze G, Schemper M. A solution to the problem of separation in logistic regression. Stat Med 2002;21:2409-19.
27. Liu H, Liu S, Lu Y, Yang Y, Wang W, Zhu L, Wei L, Wang C. Transapical transcatheter aortic valve implantation for predominant aortic regurgitation with a self-expandable valve. J Thorac Dis 2020;12:538-49.
28. Nakase M, Tomii D, Heg D, Praz F, Stortecky S, Reineke D, Samim D, Lanz J, Windecker S, Pilgrim T. Long-Term Impact of Cardiac Damage Following Transcatheter Aortic

Valve Replacement. JACC Cardiovasc Interv 2024;17:992-1003.
29. Stathogiannis K, Toutouzas K, Drakopoulou M, Michelongona A, Synetos A, Latsios G, Trantalis G, Kaitozis O, Aggeli C, Tsiamis E, Tousoulis D. The effect of mixed aortic valve disease in clinical outcomes after transcatheter aortic valve replacement. J Am Coll Cardiol 2017;69:1223.
30. Parker MW, Aurigemma GP. The Simple Arithmetic of Mixed Aortic Valve Disease: LVH + Volume Load = Trouble. J Am Coll Cardiol 2016;67:2330-3.
31. Saijo Y, Kusunose K, Takahashi T, Yamada H, Sata M, Sato K, Albakaa N, Ishizu T, Seo Y; JSE-TAVI investigators. Impact of Transcatheter Aortic Valve Replacement on Cardiac Reverse Remodeling and Prognosis in Mixed Aortic Valve Disease. J Am Heart Assoc 2024;13:e033289.
32. Chang HM, Moudgil R, Scarabelli T, Okwuosa TM, Yeh ETH. Cardiovascular Complications of Cancer Therapy: Best Practices in Diagnosis, Prevention, and Management: Part 1. J Am Coll Cardiol 2017;70:2536-51.
33. Chahine J, Kadri AN, Gajulapalli RD, Krishnaswamy A, Mick S, Perez O, Lak H, Nair RM, Montane B, Tak J, Tuzcu EM, Griffin B, Svensson LG, Harb SC, Kapadia SR. Outcomes of Transcatheter Aortic Valve Replacement in Mixed Aortic Valve Disease. JACC Cardiovasc Interv 2019;12:2299-306.
34. Stens NA, van Iersel O, Rooijakkers MJP, van Wely MH, Nijveldt R, Bakker EA, et al. Prognostic Value of Preprocedural LV Global Longitudinal Strain for Post-TAVR-Related Morbidity and Mortality: A Meta-Analysis. JACC Cardiovasc Imaging 2023;16:332-41.

Cite this article as: Chen YC, Gao YF, Zhou Z, Bo KR, Song GY, Xu L. Association between pre-procedural computed tomography angiography-based global longitudinal strain and outcomes in patients undergoing transcatheter aortic valve implantation. Quant Imaging Med Surg 2025;15(12):12684-12696. doi: 10.21037/qims-2025-841

Supplementary

Table S1 Mapping of the six-tier AR scale to conventional categories and quantitative criteria

Six-tier AR scale	Conventional categories	Key quantitative and qualitative criteria
0	None or trace	VC width (mm): not quantifiable; jet width/LVOT (%): narrow (<5); RF (%): <15
1	Mild	VC width (mm): <2; jet width/LVOT (%): narrow (5 to <15); RF (%): <15
2	Mild to moderate	VC width (mm): 2 to <4; jet width/LVOT (%): intermediate (15 to <30); RF (%): 15 to <30
3	Moderate	VC width (mm): 4 to <5; jet width/LVOT (%): intermediate (30 to <45); RF (%): 30 to <40
4	Moderate to severe	VC width (mm): 5 to <6; jet width/LVOT (%): large (45 to <60); RF (%): 40 to <50
5	Severe	VC width (mm): ≥6; jet width/LVOT (%): large (≥60); RF (%): ≥50

AR, aortic regurgitation; LVOT, left ventricular outflow tract; RF, regurgitant fraction; VC, vena contracta.

Table S2 Comparison of baseline characteristics between the final analysis patients and patients excluded due to loss to follow-up

Characteristic	Final analysis patients (n=369)	Patients lost to follow-up (n=39)	P value
Age, years	73.0 (68.0, 78.0)	75 (71.0, 80.0)	0.086
Sex (male), n (%)	207 (56.1)	18 (46.2)	0.235
BMI, kg/m^2	24.2 (22.1, 26.7)	24.3 (21.5, 26.4)	0.392
Heart rate, bmp	72.0 (68.0, 80.0)	75 (70, 82)	0.467
Diabetes, n (%)	100 (27.1)	14 (35.9)	0.244
Hypertension, n (%)	227 (61.5)	24 (61.5)	0.998
Smoking, n (%)	83 (22.5)	7 (17.9)	0.515
Alcohol, n (%)	50 (13.6)	2 (5.1)	0.203
Dyslipidemia, n (%)	180 (48.8)	16 (41.0)	0.357
BNP, pg/mL	851.0 (289.0, 2249.0)	1017 (474, 2431)	0.353
NYHA functional class III or IV, n (%)	168 (45.5)	22 (56.4)	0.195
COPD, n (%)	17 (4.6)	4 (10.3)	0.130
AF, n (%)	40 (10.8)	7 (17.9)	0.189
CAD, n (%)	206 (55.8)	19 (48.7)	0.396
Previous PCI, n (%)	54 (14.6)	8 (20.5)	0.331
Previous CABG, n (%)	3 (0.8)	2 (5.1)	0.074
LVEF, %	60.0 (53.0, 66.0)	60.0 (52.0, 65.0)	0.558
LVEDD, mm	50.0 (45.0, 58.0)	47 (44.0, 53.0)	0.067
TAPSE, mm	20.6 (19.0, 22.6)	20.0 (19.0, 20.9)	0.065
Moderate to severe AR class (Class 3–5), n (%)	161 (43.6)	12 (30.8)	0.122
CTA-GLS, %	−8.9 (−12.1, −6.6)	−8.1 (−11.1, −6.4)	0.459

Values are presented as median (interquartile range) or number (percentage). BMI, body mass index; BNP, brain natriuretic peptide; NYHA, New York Heart Association; COPD, chronic obstructive pulmonary disease; AF, atrial fibrillation; CAD, coronary artery disease; PCI, percutaneous coronary intervention; CABG, coronary artery bypass grafting; LVEF, left ventricular ejection fractions; LVEDD, left ventricular end-diastolic diameter; TAPSE, tricuspid annular plane systolic excursion; AR, aortic regurgitation; CTA-GLS, computed tomography angiography-based global longitudinal strain.

Table S3 Firth's penalized-likelihood regression analysis of clinical outcomes

Characteristic	Multivariate	
	HR (95% CI)	P value
Sex (male), n (%)	1.35 (0.48, 4.02)	0.568
Smoking, n (%)	2.37 (0.89, 6.46)	0.082
NYHA functional class III or IV, n (%)	1.85 (0.81, 4.41)	0.142
CTA-GLS, %	1.45 (1.22, 1.77)	<0.001

CI, confidence interval; CTA-GLS, computed tomography angiography-based global longitudinal strain; HR, hazard ratio; NYHA, New York Heart Association.

https://dx.doi.org/10.21037/qims-2025-841

Table S4 Results of the sensitivity Cox regression analysis using complete cases

Characteristic	Univariate		Multivariate	
	HR (95% CI)	P value	HR (95% CI)	P value
Age, years	1.01 (0.95, 1.08)	0.738		
Sex (male)	2.10 (0.73, 6.06)	0.168		
BMI, kg/m^2	1.10 (0.95, 1.27)	0.214		
Heart rate, bmp	0.96 (0.91, 1.02)	0.168		
Diabetes	0.55 (0.16, 1.94)	0.355		
Hypertension	1.06 (0.36, 3.07)	0.922		
Smoking	1.92 (0.67, 5.57)	0.227		
Alcohol	0.81 (0.18, 3.61)	0.785		
Dyslipidemia	1.16 (0.43, 3.13)	0.770		
BNP, pg/mL	1.00 (1.00, 1.00)	0.660		
NYHA functional class III or IV	2.02 (0.74, 5.47)	0.169		
Moderate to severe AR class (Class 3–5)	1.50 (0.55, 4.15)	0.430		
COPD	2.42 (0.55, 10.72)	0.243		
AF	0.59 (0.08, 4.50)	0.610		
CAD	1.41 (0.51, 3.90)	0.506		
Previous PCI	0.85 (0.19, 3.77)	0.833		
Previous CABG	2.77 (0.35, 21.86)	0.333		
LVEF, %	1.00 (0.96, 1.05)	0.971		
LVEDD, mm	0.98 (0.91, 1.05)	0.528		
TAPSE, mm	1.03 (0.89, 1.18)	0.729		
CTA-GLS, %	1.68 (1.22, 2.32)	0.001	1.68 (1.22, 2.32)	0.001
Bicuspid valve	0.76 (0.17, 3.33)	0.711		
Prothesis size	1.14 (0.88, 1.47)	0.325		
Prothesis type, mm	–*	0.988		
Pre-dilation procedure	–*	0.998		
Post-dilation procedure	1.57 (0.57, 4.30)	0.382		

*, the reference group had zero events, resulting in a non-estimable hazard ratio. BMI, body mass index; BNP, brain natriuretic peptide; CI, confidence interval; HR, hazard ratio; NYHA, New York Heart Association; AR, aortic regurgitation; COPD, chronic obstructive pulmonary disease; AF, atrial fibrillation; CAD, coronary artery disease; PCI, percutaneous coronary intervention; CABG, coronary artery bypass grafting; LVEF, left ventricular ejection fractions; LVEDD, left ventricular end-diastolic diameter; TAPSE, tricuspid annular plane systolic excursion; CTA-GLS, computed tomography angiography-based global longitudinal strain.

Table S5 Performance evaluation of models

	Sen.	Spec.	PPV	NPV
Model 1	0.65 (0.43, 0.84)	0.65 (0.60, 0.70)	0.11 (0.06, 0.18)	0.97 (0.93, 0.98)
Model 2	0.83 (0.61, 0.95)	0.65 (0.60, 0.70)	0.14 (0.09, 0.21)	0.98 (0.95, 0.99)
Model 3	0.96 (0.78, 0.99)	0.56 (0.51, 0.61)	0.13 (0.08, 0.19)	0.99 (0.97, 0.99)
P value				
Model 1 *vs*. Model 2	0.179	>0.999	0.521	0.254
Model 1 *vs*. Model 3	0.022	0.016	0.664	0.044
Model 2 *vs*. Model 3	0.346	0.016	0.808	0.380

Data in parentheses are the 95% CIs. Model 1: sex, smoking, age, and NYHA functional class III or IV; Model 2: CTA-GLS; Model 3: Model 1 + Model 2. CI, confidence interval; NPV; negative predictive value; PPV, positive predictive value; Sen., sensitivity; Spec., specificity.

https://dx.doi.org/10.21037/qims-2025-841

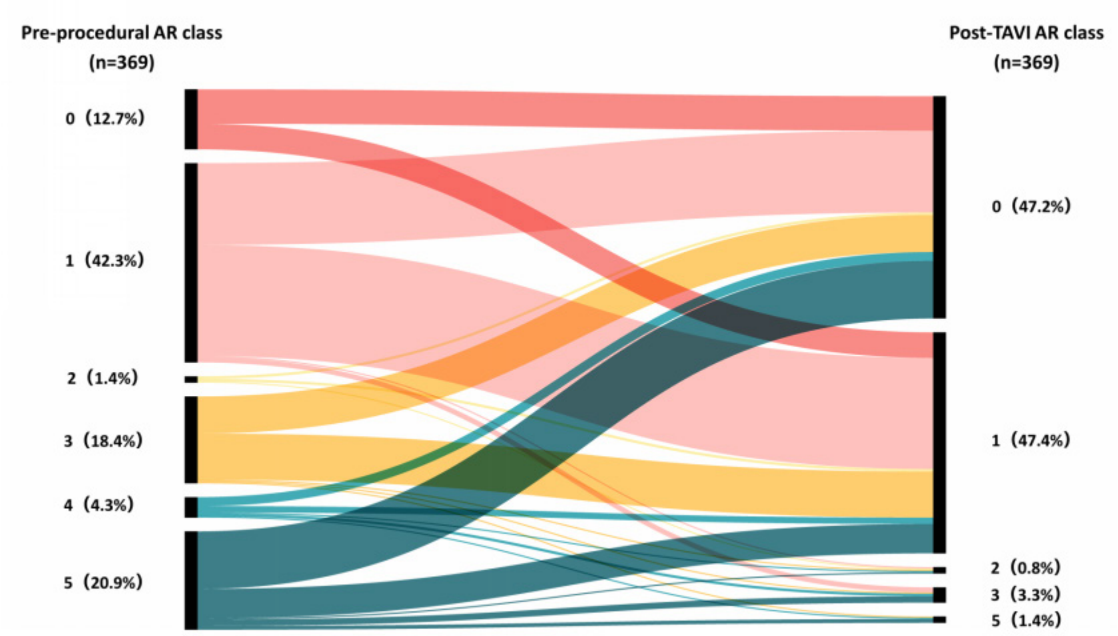

Figure S1 Sankey plot showing the percentage changes in AR class from pre-procedural to post-TAVI. AR class: 0, none or trace; 1, mild; 2, mild to moderate; 3, moderate; 4, moderate to severe; and 5, severe. AR, aortic regurgitation; TAVI, transcatheter aortic valve implantation.

https://dx.doi.org/10.21037/qims-2025-841